Materials Letters 304 (2021) 130613

Contents lists available at ScienceDirect

Materials Letters

journal homepage: www.elsevier.com/locate/matlet

Solution combustion synthesis of strontium-doped hydroxyapatite: Effect of sintering and low compaction pressure on the mechanical properties and physiological stability

D.O. Obada [a,b,i,*], K.A. Salami [a,i], A.N. Oyedeji [a,i], O.O. Fasanya [c], M.U. Suleiman [d], B.A. Ibisola [e], A.Y. Atta [f], D. Dodoo-Arhin [g], L.S. Kuburi [a], M. Dauda [a,h], E.T. Dauda [d]

[a] Department of Mechanical Engineering, Ahmadu Bello University, Zaria, Nigeria
[b] Africa Centre of Excellence on New Pedagogies in Engineering Education, Ahmadu Bello University, Zaria, Nigeria
[c] Industrial and Environmental Pollution Department, National Research Institute for Chemical Technology, Zaria, Nigeria
[d] Department of Metallurgical and Materials Engineering, Ahmadu Bello University, Zaria, Nigeria
[e] Department of Family Medicine, University College Hospital, Ibadan, Nigeria
[f] Department of Chemical Engineering, Ahmadu Bello University, Zaria, Nigeria
[g] Department of Materials Science and Engineering, University of Ghana, Legon, Ghana
[h] Air Force Institute of Technology, Nigerian Air Force Base, Kaduna, Nigeria
[i] Multifunctional Materials Laboratory, Shell Office in Mechanical Engineering, Ahmadu Bello University, Zaria, Nigeria

ARTICLE INFO

Keywords:
Bioceramics
Indentation and hardness
Phase transformation
Sintering
Microstructure

ABSTRACT

The solution combustion route was used to fabricate strontium (Sr) doped hydroxyapatite (HAp). A low compaction pressure method was adopted for pelletizing the powders (Sr-HAp) prior to physical and mechanical properties measurement. Physiological stability of the pellets was conducted by immersing in Phosphate Buffer Saline (PBS) solution for 24 h. The Sr-HAp produced a comparatively higher hardness and fracture toughness of 0.38 GPa and 0.82 MPa·$m^{1/2}$ compared with 0.20 GPa and 0.67 MPa·$m^{1/2}$ for undoped HAp. The SEM images suggested that strontium co-existed with the calcium ion in hydroxyapatite due to the presence of irregular bead-like structures on a micro-scale. The Sr-HAp pellets were stable in Phosphate Buffer Saline solution.

1. Introduction

In recent times, doping strontium on calcium phosphate to improve the material performance has gained widespread attention mostly in bone related diseases. Ceramic materials needed for bone regeneration should be bioactive, and calcium phosphates like hydroxyapatite (HAp) is widely used since it has mineral phases similar to the human bone. It is thermodynamically stable in physiological conditions due to its affinity to bond with bone. However, HAp has a very low mechanical strength making it unsuitable for load bearing applications [1,10,20–23,25]. In a way to enhance the strength and physico-chemical properties, the material is either doped or substituted with trace ions [2]. The calcium ions present are substituted with univalent, divalent and trivalent ions like Ag^{+}, Sr^{2+}, Zn^{2+}, Al^{3+}, etc., and the phosphate can also be replaced with bivalent anions like CO_3^{2-} [3–5]. Divalent $Sr^{2+}$is well known to stimulate improved bioactivity *invivo* and *invitro* for bone regeneration [6–9,19].

It has been possible to synthesize hydroxyapatite and other ceramic powders through many techniques such as microwave irradiation, solution-gelation, and solid-state synthesis [16,17,28]. Decomposition of HAp may occur at lower temperatures [18] and solid-state sintering can provide bioceramic materials that enhances osteointegration. Studies in our group have shown that solid-state sintering of HAp from natural sources at 900°C with low compaction pressures of 500 Pa and 1 MPa, produced HAp with hydroxyapatite as dominant phase, in addition to enhanced porosity and mechanical properties [10,20–23]. Therefore, in this study, we hypothesize that the inclusion of strontium into HAp using a solution-combustion (SC) assisted two-stage sintering protocol will cause a gradient in the physical and mechanical properties. The molecular level mixing and citric acid complexation of the natural hydroxyapatite and strontium precursor is capable of improving the chemical properties of the HAp produced, while urea could serve as a

* Corresponding author at: Department of Mechanical Engineering, Ahmadu Bello University, Zaria, Nigeria.
E-mail address: doobada@abu.edu.ng (D.O. Obada).

https://doi.org/10.1016/j.matlet.2021.130613
Received 22 February 2021; Received in revised form 19 June 2021; Accepted 3 August 2021
Available online 5 August 2021

Table 1
Composition and the crystallite sizes of the fabricated samples.

Sample Name		Strontium Nitrate Content (g)	Citric Acid (g)	Urea (g)	Crystallite Size (nm)	
HA-0%	20	–	7.7	2.4	r-HA	46.78
					s-HA	33.84
HA-3%	20	4.9	7.7	2.4	rHA-3%	26.15
					s-HA-3%	41.66

sacrificial fuel to supply the needed heat for the rapid conversion of the reactants to HAp. In addition, we adopted a low compaction protocol to promote densification in the Sr-HAp compacts, pre-sintering, and monitored the surface porosity with a view to enhancing the fabrication of mechanically robust Sr-HAp derived bioceramic materials.

2. Materials and methods

The chemicals used in this experiment were obtained from Sigma Aldrich. The chemical composition of the aqueous mixture for synthesizing the Sr-HAp is listed in Table 1. The hydroxyapatite powder was produced from biogenic sources as described by Obada et al, [20]. An overview of the combined protocol for the synthesis route of HAp and Sr-HAp is described in Fig. 1.

Next, the powders obtained were compacted using a low compaction pressure (1 MPa) into a circular disc (24×4 mm) for physical and mechanical measurements. The compacts were heat treated at 900°C for 2 h in the furnace with 8°C/min from room temperature to 500°C, and 2°C till 900°C. For samples' nomenclature; r-HA denotes -after solution combustion (SC) and s-HA- after heat treatment, while r-HA-3% and s-HA-3% correspond to strontium doped samples after SC and heat treatment, respectively.

The morphological examination of the materials was done using scanning electron microscope and the phases present were elucidated before and after heat treatment using Rigaku Miniflex Diffractometer followed by matching the XRD data with standard PDF cards. Crystallite sizes were calculated using the Scherer's equation [24]. The microhardness of the samples was determined with Vickers's microhardness tester. The obtained parameters from the hardness test were then used to calculate the fracture toughness, K_{1c} and the brittleness index as described in [10]. Finally, the apparent porosity was calculated using the equation as stated by Bose and Daz, [11], an Archimedes' principle-based method used to determine the apparent porosity of the samples. The swelling ratio of the scaffolds were measured using equation 1 [12]. The scaffolds were immersed in 5 ml of phosphate buffer saline (PBS, pH = 7.4) and placed in the incubator for 24 h at 37°C. The weight of the samples was taken before and after 24 h in the fluid.

$$\text{SwellingRatio}(\%) = \frac{W_w - W_d}{W_d} \times 100\% \quad (1)$$

Where W_w and W_d represent the weights of the samples before and after immersion, respectively.

3. Results and discussion

Fig. 2 shows the XRD signatures and SEM images of the doped and undoped HAp samples. The patterns of the raw data from the diffractometer were matched with the card number 96-900-2214, and samples without strontium inclusion revealed hydroxylapatite as the dominate phase. The strontium doped samples matched with card numbers 96-100-4017 and 96-900-2214. These matched diffraction data revealed strontium hydrogen phosphate and hydroxylapatite as main phases with the inclusion of tricalcium phosphates. The intense reflections for the sintered samples correspond to (002), (211), (112), (210), and (222) planes in agreement with Zhou et al [15]. The strong similarity to the XRD patterns of the undoped HAp samples demonstrates that to a certain degree, calcium ions were replaced by Sr^{2+} in the lattice of the apatite. With Sr doping, the first alteration to the XRD pattern (s-HA-3%) was the broadening of the characteristic reflections of apatite shifting it to smaller 2 theta angles in comparison to undoped HAp. With the inclusion of Sr, the sharpness of the reflection decreased due to a little mechanically induced amorphization which occured during sol–gel

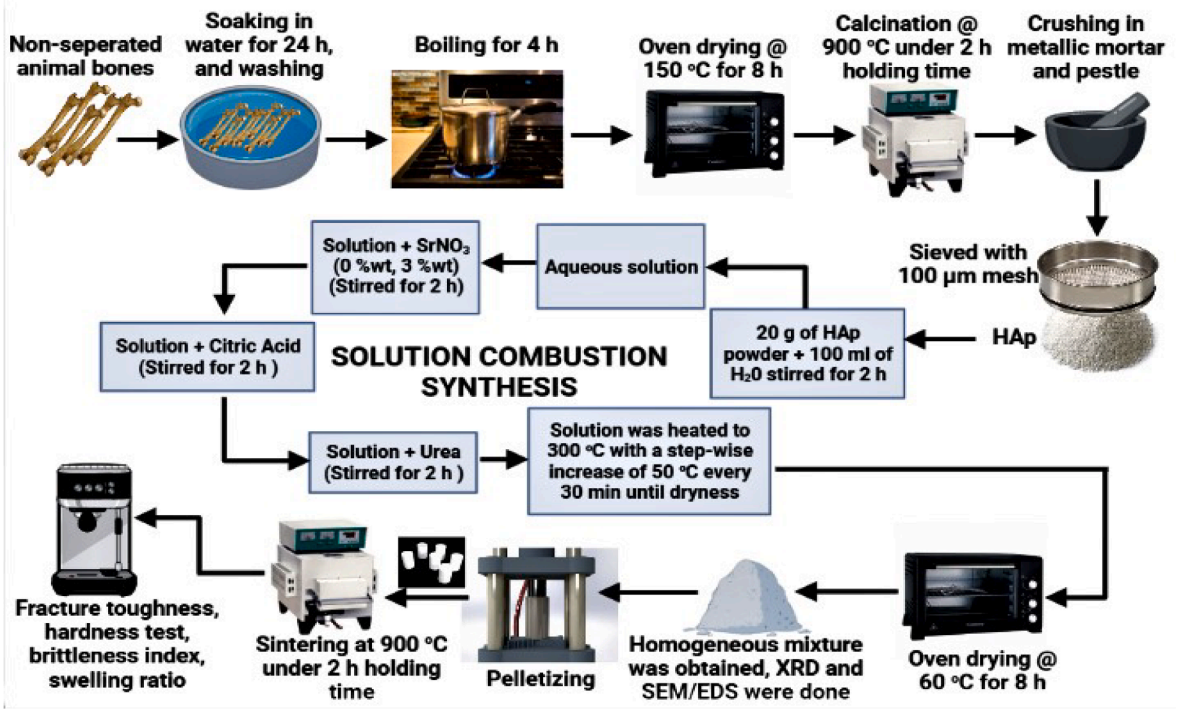

Fig. 1. Schematic for the synthesis route.

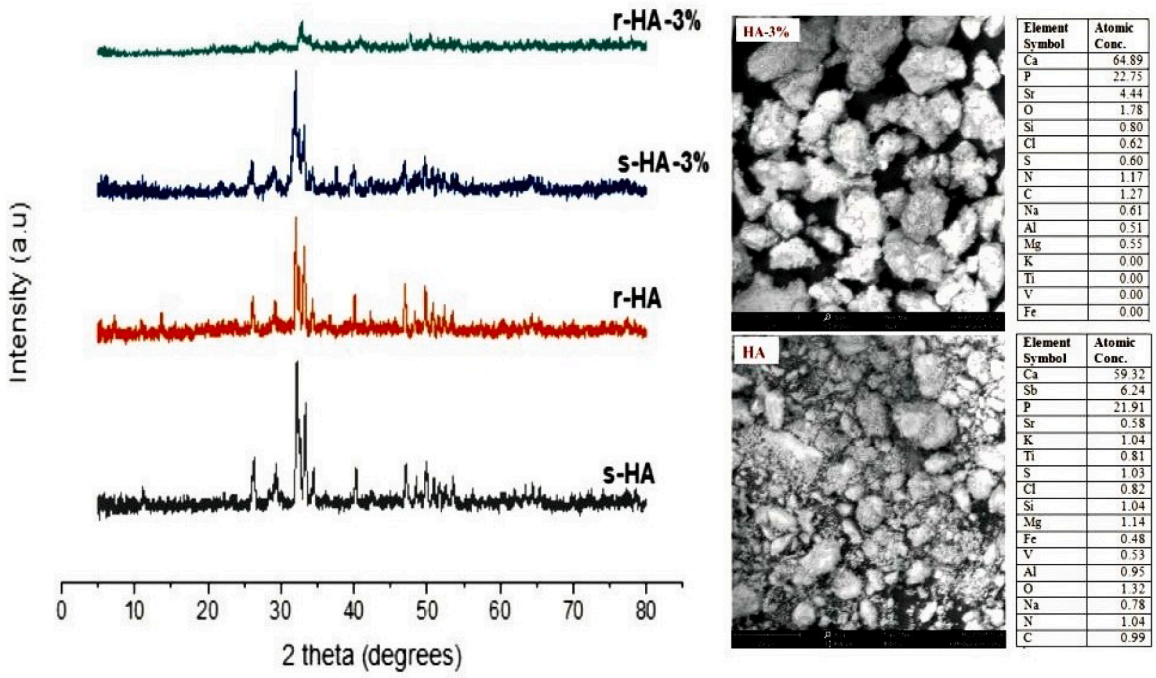

Element Symbol	Atomic Conc.
Ca	64.89
P	22.75
Sr	4.44
O	1.78
Si	0.80
Cl	0.62
S	0.60
N	1.17
C	1.27
Na	0.61
Al	0.51
Mg	0.55
K	0.00
Ti	0.00
V	0.00
Fe	0.00

Element Symbol	Atomic Conc.
Ca	59.32
Sb	6.24
P	21.91
Sr	0.58
K	1.04
Ti	0.81
S	1.03
Cl	0.82
Si	1.04
Mg	1.14
Fe	0.48
V	0.53
Al	0.95
O	1.32
Na	0.78
N	1.04
C	0.99

Fig. 2. XRD signatures and SEM/EDX of the samples.

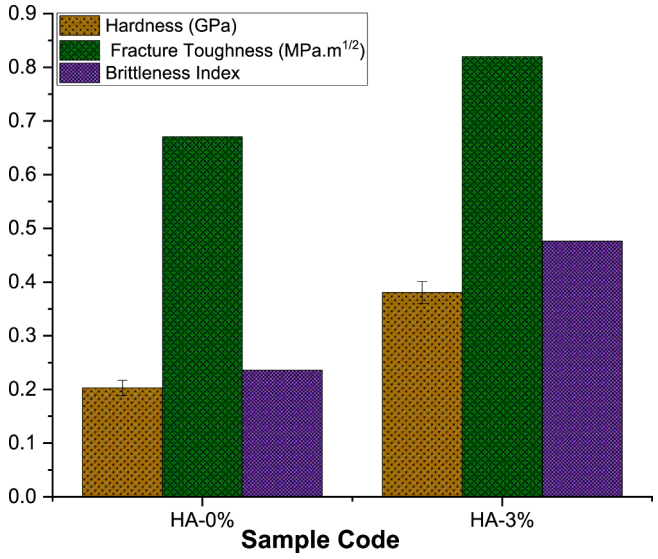

Fig. 3. Mechanical properties of the samples.

synthesis. The strontium doped HAp sample without heat treatment (r-HA-3%) shows degradation in reflections which can be ascribed to reduced bonding between the HAp and ionic dopant (Sr). Relatedly, the crystallite sizes as shown in Table 1 show that for undoped and doped samples, heat treatment caused a gradient in crystallite sizes. The increased crystallite sizes for other samples except r-HA-3% can be ascribed to enlarged crystallites due to heating.

The morphology of the sintered samples (Fig. 2) shows conspicuous agglomeration and irregular bead like structures especially for the heat-treated Sr doped sample (HA-3%). This demonstrates a possible integration of two particles co-existing. The coalescence of the particles noticed for the samples can be reduced by higher surface charges supposedly caused by solid state sintering [13,14]. The tendency to crack in physiological conditions (PBS), measured by the swelling ratio, showed that with the reduced propensity to swell, the surface pores: 32% and 39% for doped and undoped samples, respectively, were limited with reduced crack tendencies. The mechanical properties of the samples are presented in Fig. 3. Relating this to the crystallite sizes (Table 1), it is possible that the higher crystallite size of the s-HA-3% sample made its hardness value of 0.38 GPa comparatively higher and this assertion is in line with [26]. The value for hardness obtained in this study is slightly higher compared to a similar study by [27]. For humans aged between 46 and 99 years, the micro-hardness of cortical bones is in the 0.3–0.6 GPa range [20]. The micro-hardness for the s-HA-3% scaffold, as obtained in this study, was 0.38 GPa, which suggest its potentials as bone substitutes.

4. Conclusion

Sr-HAp can be synthesized using the solution combustion protocol with a controlled composition of reactants. The fluid retention capacity (swelling ratio) showed that the fabricated bioceramic materials were stable under physiological conditions. The micro-hardness of the scaffolds increased with strontium doping with a hardness value of 0.38 GPa.

CRediT authorship contribution statement

D.O. Obada: Conceptualization, Data curation, Formal analysis, Investigation, Methodology, Writing – original draft, Writing - review & editing. **K.A. Salami:** Data curation, Investigation, Writing – original draft, Writing - review & editing. **A.N. Oyedeji:** Data curation, Investigation, Writing – original draft, Writing - review & editing. **O.O. Fasanya:** Writing - review & editing. **M.U. Suleiman:** Writing - review & editing. **B.A. Ibisola:** Writing - review & editing. **A.Y. Atta:** Writing - review & editing. **D. Dodoo-Arhin:** Writing - review & editing. **L.S. Kuburi:** Formal analysis, Writing - review & editing, Supervision. **M. Dauda:** Formal analysis, Writing - review & editing, Supervision. **E.T. Dauda:** Formal analysis, Writing - review & editing, Supervision.

Declaration of Competing Interest

The authors declare that they have no known competing financial

interests or personal relationships that could have appeared to influence the work reported in this paper.

Acknowledgment

The authors wish to acknowledge TETFund Nigeria for supporting this research under grant Ref No: NRF_SETI_HSW_00714, 2020.

References

[1] W.J. Basirun, S. Baradaran, B. Nasiri-Tabrizi, Advanced 2D Materials (2016) 473–502.
[2] S. Dasgupta, A. Bandyopadhyay, S. Bose, Langmuir 26 (2010) 4958–4964.
[3] B. Nasiri-Tabrizi, E. Zalnezhad, B. Pingguan-Murphy, Basirun, S. Baradaran, Mater. Lett. 149 (2015) 100–104.
[4] S. Baradaran, E. Moghaddam, B. Nasiri-Tabrizi, W.J. Basirun, M. Mehrali, M. Sookhakian, Y. Alias, Materials Science and Engineering 49 C (2015) 656–668.
[5] A. Fakharzadeh, R. Ebrahimi-Kahrizsangi, B. Nasiri-Tabrizi, W.J. Basirun, Ceram. Int. 43 (15) (2017) 12588–12598.
[6] A. Fahami, G.W. Beall, T. Betancourt, Materials Science and Engineering 59 C (2016) 78–85.
[7] K. Tonsuaadu, K.A. Gross, L. Plūduma, M. Veiderma, J. Therm. Anal. Calorim. 110 (2) (2012) 647–659.
[8] Y.Y. Özbek, F.E. Baştan, F. Üstel, J. Therm. Anal. Calorim. 125 (2) (2016) 745–750.
[9] S. Lala, S. Brahmachari, P.K. Das, D. Das, T. Kar, S.K. Pradhan, Mater Sci Eng C. 42 (2014) 647–656.
[10] E.S. Akpan, M. Dauda, L.S. Kuburi, D.O. Obada, D. Dodoo-Arhin, Results Phys (2020).
[11] S. Bose, C. Das, Mater. Lett. 110 (2013) 152.
[12] A. Sionkowska, J. Kozłowska, Int. J. Biol. Macromol. 52 (2013) 250–259.
[13] A.R. Hanifi, M. Zazulak, T.H. Etsell, P. Sarkar, Powder Technology 231 (2012) 35–43.
[14] Beckmann W., and Beckmann W. (Ed.). Wiley-VCH, Weinheim, Germany; 2013; 75–80.
[15] H. Zhou, M. Nedley, S.B. Bhaduri, Mater. Lett. 116 (2014) 286–288.
[16] R. Ghosh, R. Sarkar, J. Aust. Ceram. Soc. 54 (1) (2018) 71–80.
[17] A.W. Reem, R. Jafer, I.S. Yahia, A.A. Al-Ghamdi, M.A. Al-ghamdi, A.M. El-Naggar, Ceram. Int. 43 (18) (2017) 17153–17159.
[18] D.J. Curran, T.J. Fleming, M.R. Towler, S. Hampshire, J. Mech. Behav. Biomed. Mater. 4 (8) (2011) 2063–2073.
[19] C.M. Mardziah, I. Sopyan, S. Ramesh, Trends Biomater, Artif. Organs 23 (2) (2009) 105–113.
[20] D.O. Obada, E.T. Dauda, J.K. Abifarin, D. Dodoo-Arhin, N.D. Bansod, Mater. Chem. Phys. 239 (2020), 122099.
[21] D.O. Obada, E.T. Dauda, J.K. Abifarin, Mater. Today:. Proc. (2020).
[22] E.S. Akpan, M. Dauda, L.S. Kuburi, D.O. Obada, Mater. Today:. Proc. (2020).
[23] E.S. Akpan, M. Dauda, L.S. Kuburi, D.O. Obada, MRS Adv. 5 (26) (2020) 1357–1366.
[24] Scherrer, P, In Kolloidchemie Ein Lehrbuch, pp. 387-409. Springer, Berlin, Heidelberg, 1912.
[25] J.K. Abifarin, D.O. Obada, E.T. Dauda, D. Dodoo-Arhin, Data in brief 26 (2019), 104485.
[26] K.A. Gross, L.M. Rodríguez-Lorenzo, Biomaterials 25 (7–8) (2004) 1385–1394.
[27] R.K. Chadha, K.L. Singh, C. Sharma, A.P. Singh, V. Naithani, Ceram. Int. 46 (1) (2020) 1091–1098.
[28] D.O. Obada, D. Dodoo-Arhin, M. Dauda, F.O. Anafi, A.S. Ahmed, O.A. Ajayi, Appl. Clay Sci. 2016 (132) (2016) 194–204.